

## **Supplemental material**

### **Materials and Methods**

#### **Construction of the rAAV vectors**

Full-length mouse VEGF-C and VEGF-D (mVEGF-Cfl and mVEGF-Dfl, respectively) were cloned into blunted MluI and NheI restriction sites of psubCMV-WPRE rAAV expression vector.<sup>1</sup> A pGA4 vector construct encoding IgK-signal peptide (21 amino acid residues) followed by the short form of mouse VEGF-C (mVEGF-Csf, residues 108-223) was synthesized by GeneArt ([www.geneart.com](http://www.geneart.com)) and cloned into the MluI restriction site of psubCMV-WPRE. The IgK-signal peptide was similarly joined to a fragment encoding residues 112-227 of human VEGF-C (hVEGF-Csf) and inserted into psubCMV-WPRE. The V146A, S179G and C137A mutants of hVEGF-Csf were produced by site-directed mutagenesis. The mouse interleukin-3 signal peptide (33 amino acid residues) was fused to the short form of mouse VEGF-D (mVEGF-Dsf, residues 94-210) or human VEGF-D (hVEGF-Dsf, residues 89-205) by PCR amplification. The resulting fragment was then cloned into the MluI site of psubCMV-WPRE. rAAV vectors encoding human VEGF-A<sub>165</sub> isoform (VEGF<sub>165</sub>) and the chimeric factor CAC have been described previously.<sup>2</sup>

#### **Recombinant AAV vector preparation**

The recombinant AAVs (rAAVs, serotype 8) were produced as described previously<sup>3,4</sup> with the following modifications. Instead of pDG plasmid, a combination of adenovirus helper plasmid pBS-E2A-VA-E4<sup>5</sup> and the serotype helper plasmid p5e18-VD2/8<sup>6</sup> were employed. The rAAV preparations were purified by ultracentrifugation using an iodixanol step gradient.<sup>7</sup> The rAAV-containing layer was

directly used for determination of virus titer by real-time PCR, for *in vitro* testing and mouse injections.

### **MTT cell survival assay and analysis of protein expression by IP**

VEGFR-2/BaF3 and VEGFR-3/BaF3 cells are derived from the IL-3-dependent mouse pro-B cell line, BaF3<sup>8</sup>. These express a chimeric receptor consisting of the extracellular domain of mouse VEGFR-2<sup>9,10</sup> or human VEGFR-3 fused in-frame to the transmembrane and intracellular domains of mouse erythropoietin receptor.<sup>11</sup> In interleukin-3-deficient media, both cells can be rescued by the addition of the respective ligands. Supernatants containing the growth factors of interest were produced by transfection of 293T cells using jetPEI transfection reagent (Polyplus-transfection). Proteins were metabolically labeled with [<sup>35</sup>S]Cys/Met (Promix, NEN Radiochemicals). 50 µl volumes of serial dilutions of supernatants, as well as positive and negative controls, were applied in the wells of 96-well plates in triplicate. Subsequently, 20,000 VEGFR/BaF3 cells in 50 µl were added to each well and the cells were incubated at 37°C for 48 h. MTT substrate was added, and the cells were incubated at 37°C for 2 h. Lysis buffer (10% SDS, 10 mM HCl) was added, and the plates were incubated at 37°C overnight for color development. Quantification was done by absorbance at 540 nm. For analysis of protein expression, supernatants containing [<sup>35</sup>S]-labelled growth factors were precipitated with VEGFR-2-Ig or VEGFR-3-Ig and Protein A Sepharose, and analysed using SDS-PAGE and autoradiography.

### **Protein purification**

For the *in vitro* binding assays, hVEGF-Csf was prepared as described previously<sup>12</sup>. C-terminal 6xHis-tagged hVEGF-Csf C137A mutant (residues 112-215) was expressed in Sf9 insect cells using the Bac-to-Bac baculovirus expression system (Gibco). Soluble VEGFR-3 (domains 1-3 fused to IgGFc) was prepared as described previously.<sup>13</sup> Soluble VEGFR-2 (domains 2-3 fused to IgGFc) was prepared similarly except that it was expressed in Sf9 insect cells using the Bac-to-Bac baculovirus expression system (Gibco). The cDNA coding for the human VEGF<sub>165</sub> isoform was inserted into the pMT/V5-HisA expression vector (Invitrogen). VEGF<sub>165</sub> was purified from conditioned supernatant from S2 cells stably transfected with the resulting vector (pMT-hVEGF<sub>165</sub>) by heparin affinity chromatography followed by cation exchange chromatography and gel filtration.

### **Isothermal titration calorimetry**

Calorimetric titrations of the soluble VEGFR-3 with hVEGF-Csf C137A, or WT (wild type), were carried out at 25°C using a VP-ITC calorimeter (MicroCal). Prior to titration, the protein samples were degassed for 5 min. 10 mM HEPES, 100 mM sodium chloride, pH 7.5 was used to control for heat dilution effects. VEGFR-3 was used in the calorimeter cell at a concentration of 6 µM, and the VEGF-Csf ligands in the syringe at a concentration of 0.14-0.17 mM. Data were processed using MicroCal Origin 7.0 software.

### **VEGFR-2 and VEGFR-3 ELISA assays**

For the enzyme linked immunoassays, hVEGF-Csf at 0.8 µg/ml (VEGFR-3 assay) and VEGF<sub>165</sub> at 0.9 µg/ml (VEGFR-2 assay) in PBS were used to coat MaxiSorp immunoplates (Thermo Fischer Scientific). To determine the relative binding

affinities, 0.2 µg/ml of soluble human VEGFR-2-Fc was preincubated with 10 pM to 10 µM hVEGF-Csf C137A (or hVEGF-Csf) in 0.5 % BSA and 0.1 % Tween-20, and then transferred onto the VEGF<sub>165</sub> plate for the competition assay. Similarly, soluble 0.3 µg/ml human VEGFR-3-Fc was preincubated with hVEGF-Csf C137A (or hVEGF-Csf) and then transferred onto the hVEGF-Csf plate. After extensive washing with PBS, 0.1 % Tween-20, the bound receptor was quantified by HRP-conjugated anti human antibody (DakoCytomation) together with SureBlue peroxidase substrate (KPL). To determine the IC<sub>50</sub> values for the one-site binding model, nonlinear regression analysis was performed using Prism v3.02 (GraphPad Software).

### **Immunohistochemistry**

Muscles were isolated and frozen in O.C.T (TissueTek, Sakura Finetek). Cryosections (8 µm) were cut, acetone-fixed, and immunostained using the following antibodies: rat anti-PECAM-1 (Pharmingen), rat anti-CD45 (Pharmingen), rat F4-80 (Serotec), mouse anti-smooth muscle actin (SMA)-Cy3 (Sigma), rabbit anti-human PROX-1 and rabbit anti-mouse LYVE-1 antisera, and Hoechst 33258 for DNA staining. Secondary antibodies were Alexa Fluor-conjugated (Molecular Probes, Eugene, OR). Microvessel area density was quantified using ImageJ software (NIH).

### ***In vivo* Doppler ultrasound measurements of perfusion in transduced muscles**

Doppler ultrasound was used to analyze blood perfusion in the transduced *t.a.* muscles of anesthetized mice two weeks post-transduction. Mice were anesthetized with xylazine (Rompun, Bayer)-ketamine (Ketalar, Pfizer) and their hindlegs were shaved. For analysis, the mouse was gently fixed on a platform heated to 36°C and the analysed area was covered by ultrasound gel. Muscle area was scanned using the

VEVO 770 Micro-Ultrasound System (VisualSonics Inc.). B-Mode images were acquired to confirm anatomic boundaries of target muscle in Doppler images. To evaluate the potential effect of heart rate on Doppler signals, electrocardiographic (ECG) measurements were performed immediately following Doppler analysis. No significant differences in heart rate were observed between the mice (data not shown). Image stacks were generated by three-dimensional scanning. The fraction of surface area covered by perfused blood vessels was quantified as "perfused vessels (% of area)" in Doppler images using the VisualSonics software. The region of interest was manually restricted to the tibialis anterior muscle.

#### **FITC-lectin microlymphography**

2  $\mu$ l of FITC-lectin (Vector Laboratories) was injected into the lower (distal) region of the *t.a.* muscle of anesthetized mice. After 45 min the mice were sacrificed, and the muscles were prepared, photographed, frozen in O.C.T, and sectioned. Parallel sections were stained with antibodies recognizing markers of lymphatic endothelium, PROX-1 or LYVE-1, followed by incubation with secondary antibodies conjugated with Alexa Fluor-594.

#### **Supplemental figure legends**

**Online Figure I. A. Alignment of VEGF-C sequences.** The VEGF-C sequences of the different vertebrates indicated show considerable conservation in the region of proteolytically processed, mature human VEGF-C (hVEGF-Csf). Residues differing between species are marked in red. Species: Human – homo sapiens; monkey – macaca mulatta (rhesus monkey); dog – canis lupus familiaris; cow – bos taurus;

mouse – mus musculus; rat – rattus norvegicus; chicken – gallus gallus. **B. Schematic representation of the VEGF proteins used in this study.** The CAC protein consist of the N- and C-terminal propeptide domains (NT and CT, respectively) of human VEGF-C fused to the VEGF homology domain (VHD, amino acid residues 37 to 135) of human VEGF-A.<sup>2</sup> Growth factor abbreviations are described in the legend of Figure 1.

**Online Figure II. Receptor activation by various forms of VEGF-C and VEGF-D.** MTT cell survival assay was carried out using VEGFR-3/BaF3 and VEGFR-2/BaF3 cells as described in Materials and Methods. Supernatant produced by empty vector-transfected 293T-derived cells was used as a mock control. Interleukin-3 (IL-3, 2 ng/ml) was used as a positive control for cellular viability/proliferation. Note that all VEGF-D forms are inactive, when used in the concentrations corresponding to the highest VEGF-C (either sf or fl) concentrations shown (for example, compare OD540 readings for VEGF-D and VEGF-C stimulation of VEGFR-2/BaF3 and VEGFR-3/BaF3 cells obtained at 2.5% of and 0.3% ligand concentrations, respectively). Statistically significant differences between the activities of the various growth factor forms over range of sub-saturating concentrations are indicated by the appropriately colored asterisks and brackets (\* indicates  $P < 0.05$ ).

**Online Figure III. Blood vascular, lymphatic, endothelial and smooth muscle immunostaining two weeks after transduction of the indicated vectors into *t.a.* muscles of ICR mice.** Double-immunostaining of the indicated antigens were carried out using frozen muscle sections. **A.** Quantification of the immunostaining as described in Materials and Methods. **B.** Representative images obtained from the

mVEGF-Csf-, mVEGF-Dsf-, and HSA vector-transduced muscle samples. Note that in the ICR mouse strain the inflammatory (CD45-positive) cells are more numerous also in the negative control (HSA), in contrast to the other two mouse strains tested. \* - statistically significant ( $P < 0.05$ ) differences between experimental groups and control (HSA).

**Online Figure IV. Double immunostaining of transduced muscles for PECAM-1 and SMA.** Samples are described in the legend of Figure 3. Quantification of the immunostaining is shown in Figure 3A.

**Online Figure V. Mouse VEGF-Dsf induces a strong paracrine angiogenic effect in skeletal muscle.** PECAM-1 immunostaining labels blood vessels and shows a rich vascular network surrounding myofibres positive for mVEGF-Dsf (mDsf). The scale bar indicates 50  $\mu\text{m}$ .

## References

1. Paterna JC, Moccetti T, Mura A, Feldon J, Bueler H. Influence of promoter and WHV post-transcriptional regulatory element on AAV-mediated transgene expression in the rat brain. *Gene Ther.* 2000;7:1304-1311.
2. Keskitalo S, Tammela T, Lyytikka J, Karpanen T, Jeltsch M, Markkanen J, Yla-Herttuala S, Alitalo K. Enhanced capillary formation stimulated by a chimeric vascular endothelial growth factor/vascular endothelial growth factor-C silk domain fusion protein. *Circ Res.* 2007;100:1460-1467.

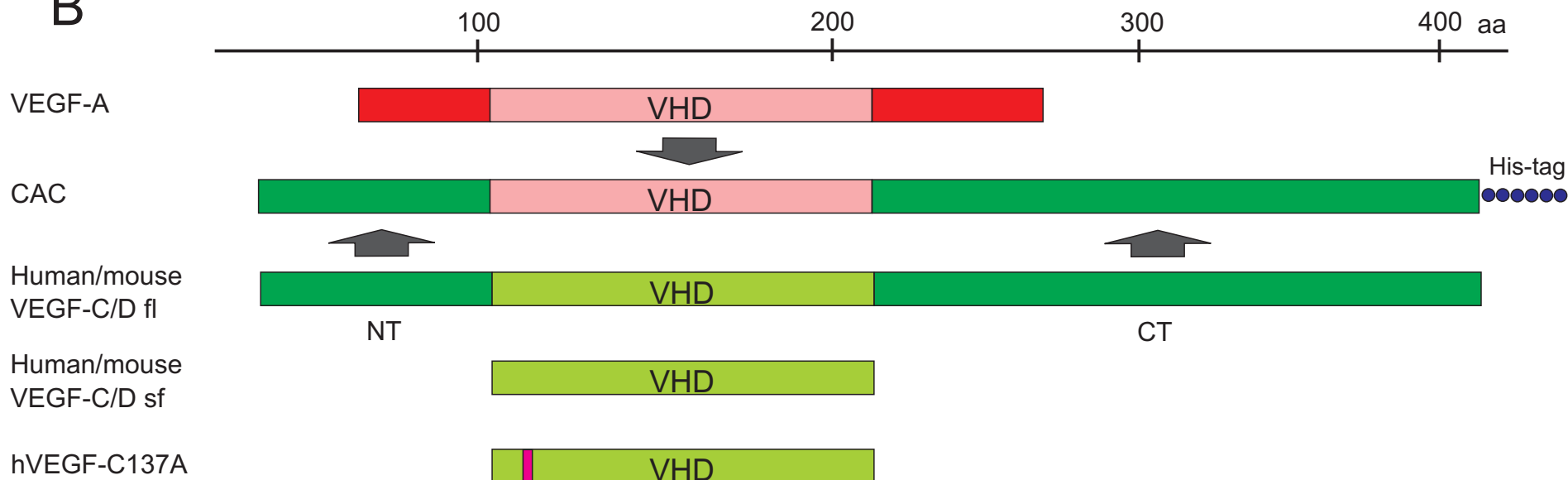
3. Grimm D, Kern A, Rittner K, Kleinschmidt JA. Novel tools for production and purification of recombinant adenoassociated virus vectors. *Hum Gene Ther.* 1998;9:2745-2760.
4. Pajusola K, Kunnapuu J, Vuorikoski S, Soronen J, Andre H, Pereira T, Korpisalo P, Yla-Herttuala S, Poellinger L, Alitalo K. Stabilized HIF-1alpha is superior to VEGF for angiogenesis in skeletal muscle via adeno-associated virus gene transfer. *FASEB J.* 2005;19:1365-1367.
5. Jalkanen J, Leppanen P, Pajusola K, Narvanen O, Mahonen A, Vahakangas E, Greaves DR, Bueler H, Yla-Herttuala S. Adeno-associated virus-mediated gene transfer of a secreted decoy human macrophage scavenger receptor reduces atherosclerotic lesion formation in LDL receptor knockout mice. *Mol Ther.* 2003;8:903-910.
6. Gao GP, Alvira MR, Wang L, Calcedo R, Johnston J, Wilson JM. Novel adeno-associated viruses from rhesus monkeys as vectors for human gene therapy. *Proc Natl Acad Sci U S A.* 2002;99:11854-11859.
7. Zolotukhin S, Byrne BJ, Mason E, Zolotukhin I, Potter M, Chesnut K, Summerford C, Samulski RJ, Muzyczka N. Recombinant adeno-associated virus purification using novel methods improves infectious titer and yield. *Gene Ther.* 1999;6:973-985.
8. Bernardi P, Patel VP, Lodish HF. Lymphoid precursor cells adhere to two different sites on fibronectin. *J Cell Biol.* 1987;105:489-498.
9. Achen MG, Jeltsch M, Kukk E, Makinen T, Vitali A, Wilks AF, Alitalo K, Stacker SA. Vascular endothelial growth factor D (VEGF-D) is a ligand for the tyrosine kinases VEGF receptor 2 (Flk1) and VEGF receptor 3 (Flt4). *Proc Natl Acad Sci U S A.* 1998;95:548-553.

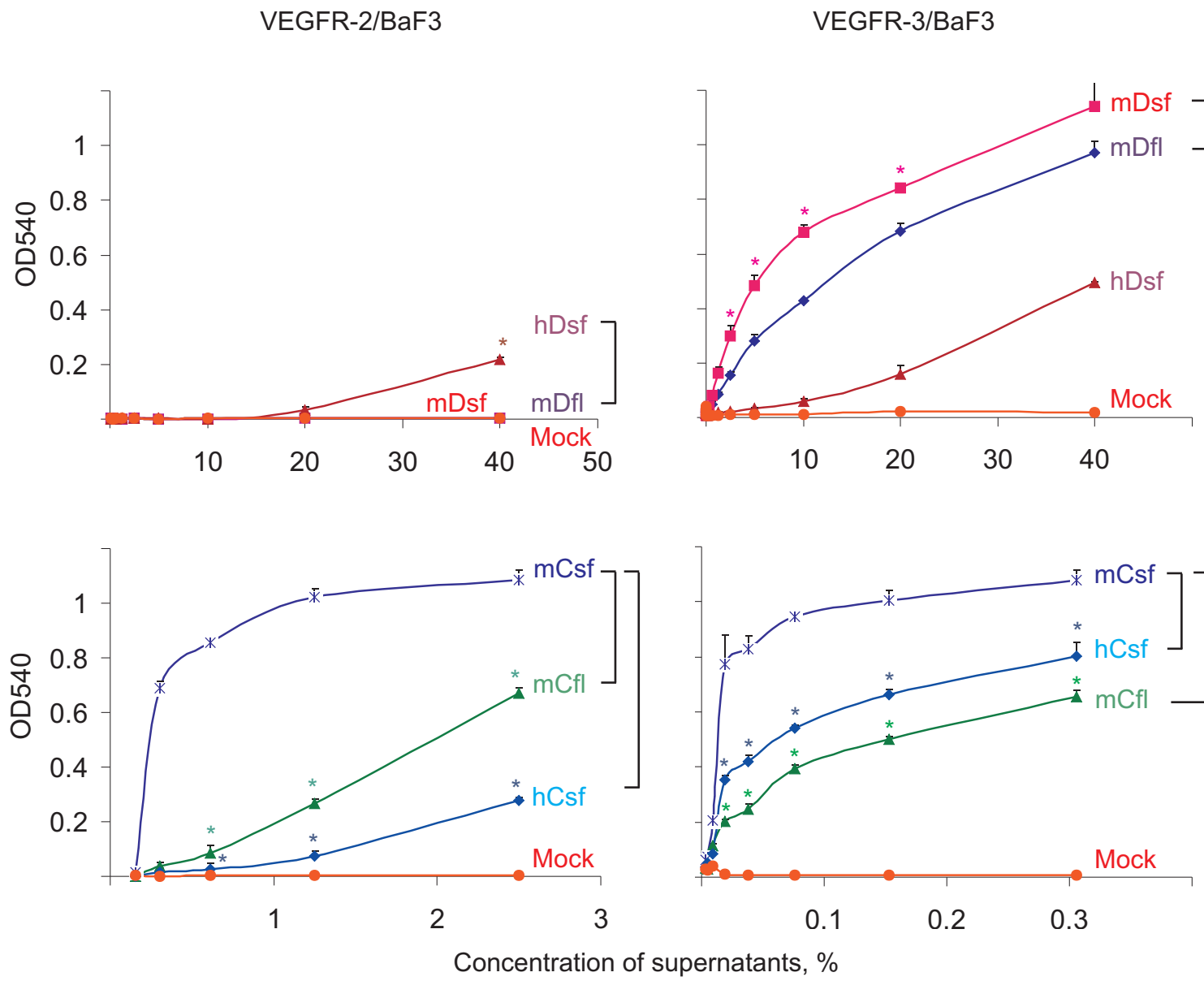
10. Stacker SA, Vitali A, Caesar C, Domagala T, Groenen LC, Nice E, Achen MG, Wilks AF. A mutant form of vascular endothelial growth factor (VEGF) that lacks VEGF receptor-2 activation retains the ability to induce vascular permeability. *J Biol Chem.* 1999;274:34884-34892.
11. Achen MG, Roufail S, Domagala T, Catimel B, Nice EC, Geleick DM, Murphy R, Scott AM, Caesar C, Makinen T, Alitalo K, Stacker SA. Monoclonal antibodies to vascular endothelial growth factor-D block its interactions with both VEGF receptor-2 and VEGF receptor-3. *Eur J Biochem.* 2000;267:2505-2515.
12. Karpanen T, Heckman CA, Keskitalo S, Jeltsch M, Ollila H, Neufeld G, Tamagnone L, Alitalo K. Functional interaction of VEGF-C and VEGF-D with neuropilin receptors. *FASEB J.* 2006;20:1462-1472.
13. Makinen T, Jussila L, Veikkola T, Karpanen T, Kettunen MI, Pulkkanen KJ, Kauppinen R, Jackson DG, Kubo H, Nishikawa S, Yla-Herttuala S, Alitalo K. Inhibition of lymphangiogenesis with resulting lymphedema in transgenic mice expressing soluble VEGF receptor-3. *Nat Med.* 2001;7:199-205.

A

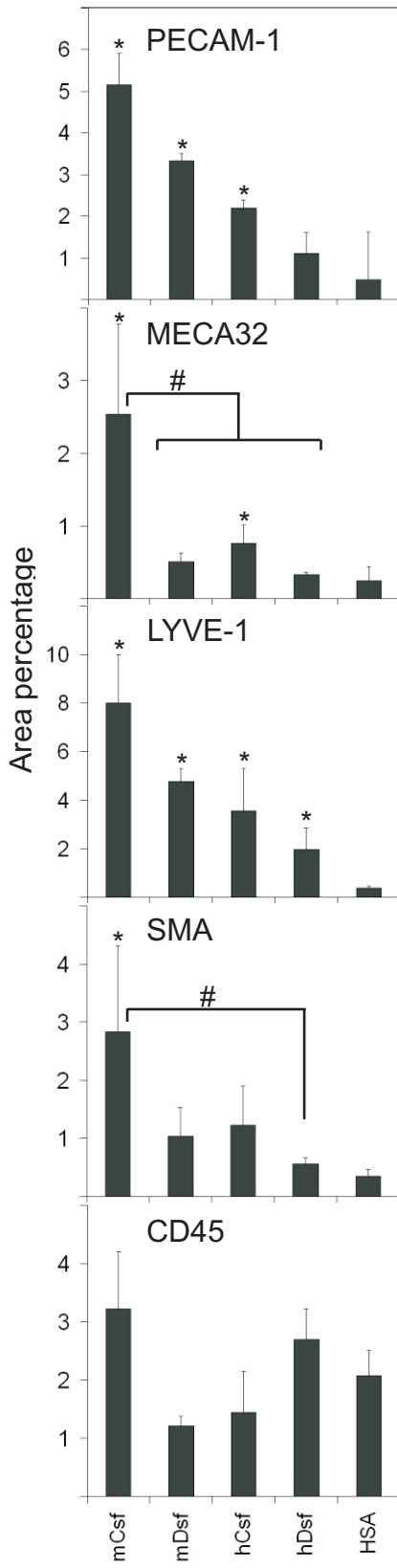
Human AHYNTEILKSIDNEWRKTQCMPEVCI DVGKEFGVATNTFFKPPCVSVYRCGGCCNSEGLQCMN TSTSYLSKTLFEITVPLSQGPKPVTISFANHTSRCMSKLDVYRQVHSIIRR  
 Monkey AHYNAEILKSIDNEWRKTQCMPEVCI DVGKEFGVATNTFFKPPCVSVYRCGGCCNSEGLQCMN TSTSYLSKTLFEITVPLSQGPKPVTISFANHTSRCMSKLDVYRQVHSIIRR  
 Dog AHYNAEILKSIDNEWRKTQCI PREVCI DVGKEFGAATNTFFKPPCVSVYRCGGCCNSEGLQCMN TSTSHLSKTLFEITVPLSQGPKPVTISFANHTSRCMSKLDVYRQVHSIIRR  
 Cow AHYNTEILRSIDNEWRKTQCMPEVCI DVGKEFGAATNTFFKPPCVSVYRCGGCCNSEGLQCMN TSTSYLSKTLFEITVPLSQGPKPVTISFANHTSRCMSKLDVYRQVHSIIRR  
 Mouse AHYNTEILKSIDNEWRKTQCMPEVCI DVGKEFGAATNTFFKPPCVSVYRCGGCCNSEGLQCMN TSTGYLSKTLFEITVPLSQGPKPVTISFANHTSRCMSKLDVYRQVHSIIRR  
 Rat AHYNTEILKSIDNEWRKTQCMPEVCI DVGKEFGAATNTFFKPPCVSVYRCGGCCNSEGLQCMN TSTGYLSKTLFEITVPLSQGPKPVTISFANHTSRCMSKLDVYRQVHSIIRR  
 Chicken AHYNAEILKSIDTEWRKTQCMPEVCI DVGKEFGATNTFFKPPCVSIYRCGGCCNSEGLQCMN ISTNYLSKTLFEITVPLSHGPKPVTISFANHTSRCMSKLDVYRQVHSIIRR

B

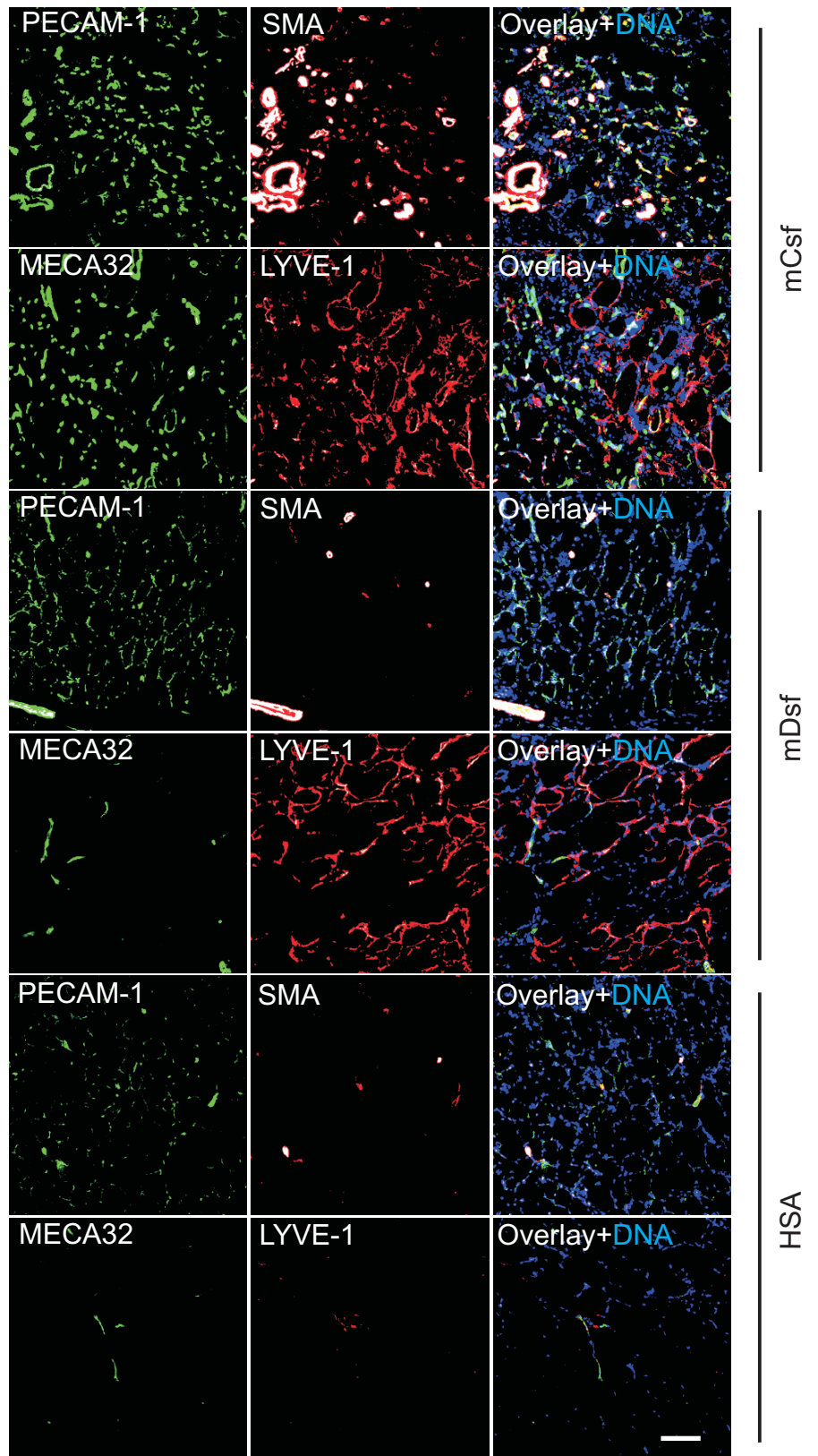


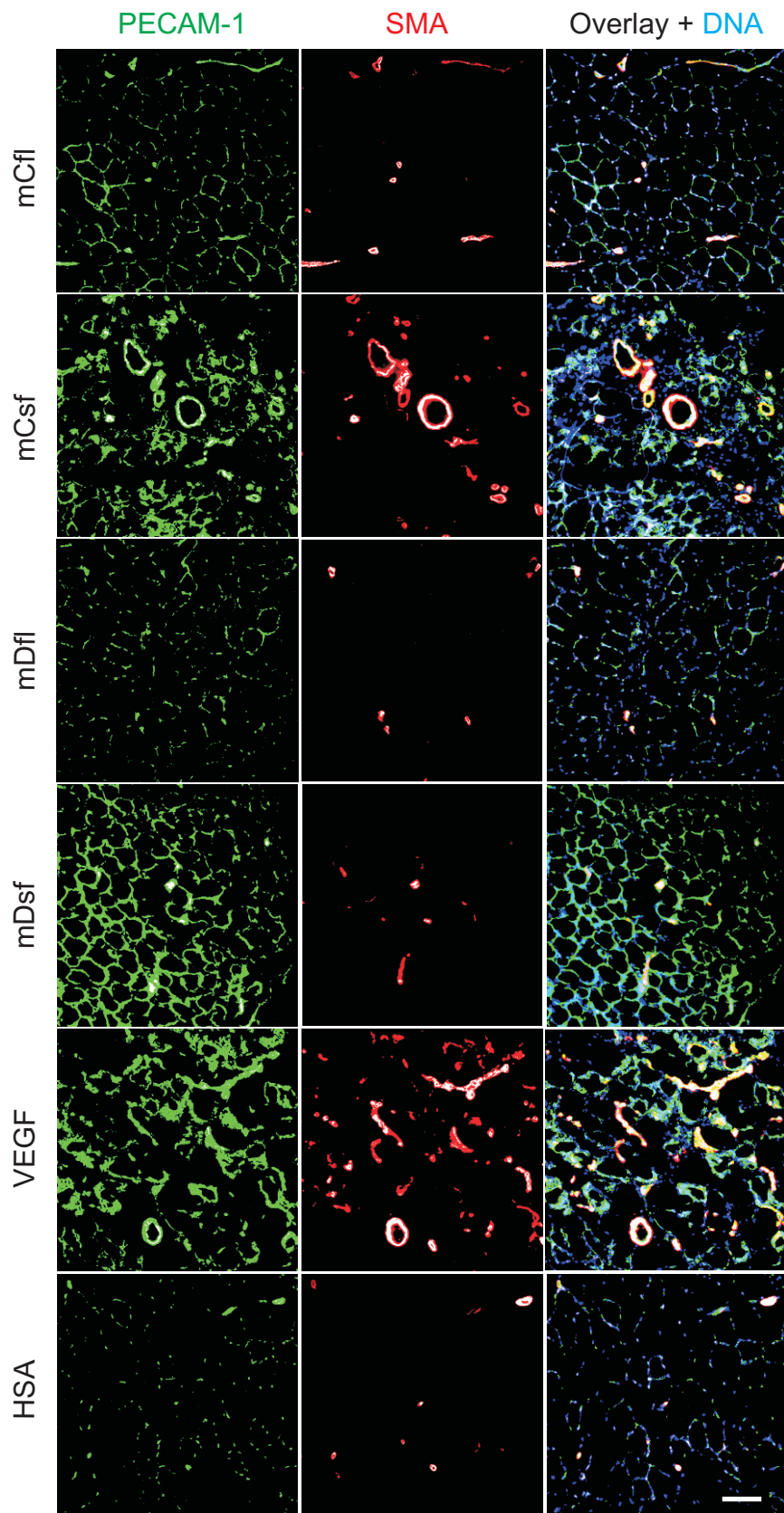


A

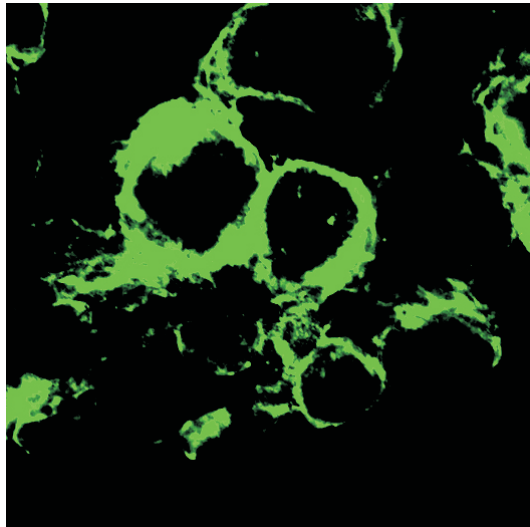


B

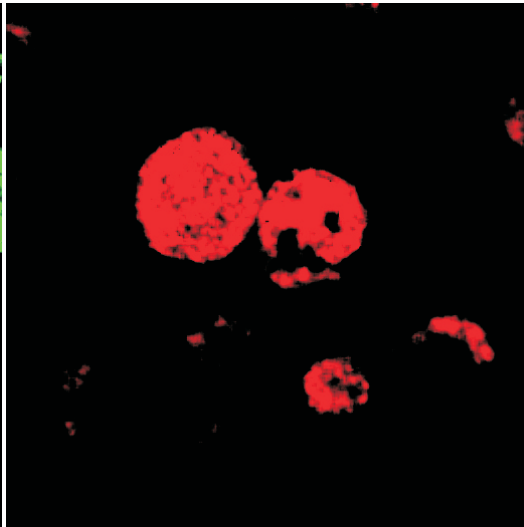




PECAM-1



mDsf



Overlay + DNA

